AGU PUBLICATIONS

Paleoceanography

RESEARCH ARTICLE
10.1002/2016PA003073

Key Points:
- $\delta^{18}O_{sw}$-salinity relationship varies across tropical Pacific
- $\delta^{18}O_{sw}$ covaries with precipitation in the western tropical Pacific
- Local $\delta^{18}O_{sw}$-salinity relationship impacts carbonate $\delta^{18}O$ variance in western tropical Pacific

Supporting Information:
- Supporting Information S1
- Data S1

Correspondence to:
J. L. Conroy,
jconro@illinois.edu

Citation:
Conroy, J. L., D. M. Thompson, K. M. Cobb, D. Noone, S. Rea, and A. N. Legrande (2017), Spatiotemporal variability in the $\delta^{18}O$-salinity relationship of seawater across the tropical Pacific Ocean, *Paleoceanography*, *32*, 484–497, doi:10.1002/2016PA003073.

Received 13 DEC 2016
Accepted 6 APR 2017
Accepted article online 20 APR 2017
Published online 13 MAY 2017

Spatiotemporal variability in the $\delta^{18}O$-salinity relationship of seawater across the tropical Pacific Ocean

Jessica L. Conroy[1,2], Diane M. Thompson[3], Kim M. Cobb[4], David Noone[5], Solanda Rea[6], and Allegra N. Legrande[7]

[1]Department of Geology, University of Illinois at Urbana–Champaign, Champaign, Illinois, USA, [2]Department of Plant Biology, University of Illinois at Urbana–Champaign, Urbana, Illinois, USA, [3]Earth and Environment, Boston University, Boston, Massachusetts, USA, [4]School of Earth and Atmospheric Sciences, Georgia Institute of Technology, Atlanta, Georgia, USA, [5]College of Earth, Ocean, and Atmospheric Sciences, Oregon State University, Corvallis, Oregon, USA, [6]Charles Darwin Research Foundation, Puerto Ayora, Ecuador, [7]NASA Goddard Institute for Space Studies, Columbia University, New York, New York, USA

Abstract The relationship between salinity and the stable oxygen isotope ratio of seawater ($\delta^{18}O_{sw}$) is of utmost importance to the quantitative reconstruction of past changes in salinity from $\delta^{18}O$ values of marine carbonates. This relationship is often considered to be uniform across water masses, but the constancy of the $\delta^{18}O_{sw}$-salinity relationship across space and time remains uncertain, as $\delta^{18}O_{sw}$ responds to varying atmospheric vapor sources and pathways, while salinity does not. Here we present new $\delta^{18}O_{sw}$-salinity data from sites spanning the tropical Pacific Ocean. New data from Palau, Papua New Guinea, Kiritimati, and Galápagos show slopes ranging from 0.09 ‰/psu in the Galápagos to 0.32‰/psu in Palau. The slope of the $\delta^{18}O_{sw}$-salinity relationship is higher in the western tropical Pacific versus the eastern tropical Pacific in observations and in two isotope-enabled climate model simulations. A comparison of $\delta^{18}O_{sw}$-salinity relationships derived from short-term spatial surveys and multiyear time series at Papua New Guinea and Galápagos suggests spatial relationships can be substituted for temporal relationships at these sites, at least within the time period of the investigation. However, the $\delta^{18}O_{sw}$-salinity relationship varied temporally at Palau, likely in response to water mass changes associated with interannual El Niño–Southern Oscillation (ENSO) variability, suggesting nonstationarity in this local $\delta^{18}O_{sw}$-salinity relationship. Applying local $\delta^{18}O_{sw}$-salinity relationships in a coral $\delta^{18}O$ forward model shows that using a constant, basinwide $\delta^{18}O_{sw}$-salinity slope can both overestimate and underestimate the contribution of $\delta^{18}O_{sw}$ to carbonate $\delta^{18}O$ variance at individual sites in the western tropical Pacific.

1. Introduction

The stable oxygen isotopic composition of seawater (henceforth $\delta^{18}O_{sw}$) and salinity are correlated due to the similar influence of freshwater fluxes on both variables, although $\delta^{18}O_{sw}$ can also respond to changes in the $\delta^{18}O$ value of atmospheric moisture sources. $\delta^{18}O_{sw}$ often serves as a proxy for salinity, a variable critical for understanding past ocean circulation and structure as well as the hydrologic cycle [e.g., *Adkins et al.*, 2002; *Durack et al.*, 2012; *Leech et al.*, 2013; *Nurhati et al.*, 2011; *Roberts et al.*, 2016; *Rustic et al.*, 2015; *Stott et al.*, 2004]. Due to the nature of this relationship, $\delta^{18}O$ measurements from marine carbonates, namely, corals, foraminifera, and mollusks, provide a source of important information on past salinity variability, especially when the influence of temperature on carbonate $\delta^{18}O$ values can be independently assessed, such as with Sr/Ca in corals or Mg/Ca in foraminifera [e.g., *Alibert and McCulloch*, 1997; *Beck et al.*, 1997; *Lea et al.*, 1999; *Rustic et al.*, 2015], provided there is no salinity overprint on elemental ratios [e.g., *Kısakürek et al.*, 2008].

Although variability in proxy values for $\delta^{18}O_{sw}$ in the mixed layer is often inferred to be a result of freshwater fluxes (precipitation and evaporation), horizontal advection, vertical entrainment, and diffusion may also play important roles in shaping the $\delta^{18}O_{sw}$-salinity relationship, especially at finer spatial scales [*Stevenson et al.*, 2015]. Such processes are essential for closing the mixed layer salinity budget across the tropical Pacific [*Hasson et al.*, 2013]. Understanding how these multiple influences converge to produce $\delta^{18}O_{sw}$ variability as well as variability in the $\delta^{18}O_{sw}$-salinity relationship is a critical task that to date remains incomplete.

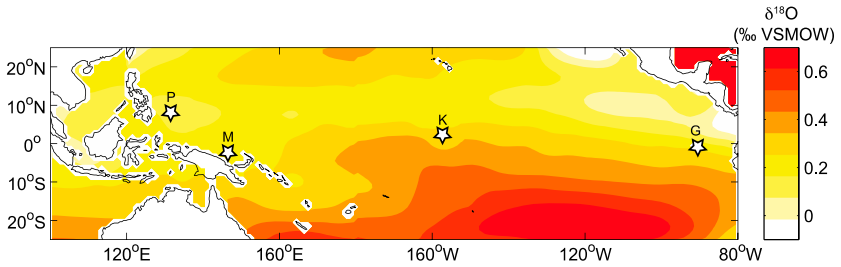

Figure 1. Map of study sites, indicated by stars. P: Palau, M: Manus, K: Kiritimati, G: Galápagos. Contour map of interpolated $\delta^{18}O_{sw}$ from *LeGrande and Schmidt* [2006].

Previous work has challenged the fundamental assumption that the $\delta^{18}O_{sw}$-salinity relationship is constant across space and time, given variability in freshwater fluxes and advection [*Rohling and Bigg*, 1998]. Most notably, a compilation of spatial observations indicates differences in the $\delta^{18}O_{sw}$-salinity relationship across large water masses, such as between the tropical Pacific and the extratropical Pacific [*LeGrande and Schmidt*, 2006]. These relationships are critical for converting proxy $\delta^{18}O_{sw}$ values to salinity and quantitatively reconstructing climate. The utility of the modern $\delta^{18}O_{sw}$-salinity relationship highlights the need for a thorough investigation of this relationship at specific proxy locales, rather than assuming constant relationships across large regions of the ocean. Additionally, the spatial $\delta^{18}O_{sw}$-salinity relationship is often substituted for the temporal relationship when applied to $\delta^{18}O_{sw}$ proxies. This assumption, that modern spatial relationships approximate temporal relationships, has not been adequately tested with observations. Model-based inquiries into the robustness of this assumption show grave concerns, revealing variable $\delta^{18}O_{sw}$-salinity relationships across space and time [*Holloway et al.*, 2016], particularly on millennial and longer time scales [*LeGrande and Schmidt*, 2011].

The contribution of salinity and temperature to carbonate $\delta^{18}O$ can also be explored through proxy system modeling of marine carbonate $\delta^{18}O$ [*Evans et al.*, 2013]. In such process-based models, where temperature and salinity are used to calculate carbonate $\delta^{18}O$ for comparison to existing proxy $\delta^{18}O$ records [*Thompson et al.*, 2011], salinity is typically substituted for $\delta^{18}O_{sw}$ using the existing, empirically derived $\delta^{18}O_{sw}$-salinity relationship for specific ocean regions [*LeGrande and Schmidt*, 2006] due to the limited coverage of $\delta^{18}O_{sw}$ data. Thus, proxy system models of marine carbonate $\delta^{18}O$ may also be improved through a more mature understanding of the $\delta^{18}O_{sw}$-salinity relationship across space and time.

Here we present new temporal and spatial data sets of $\delta^{18}O_{sw}$ and sea surface salinity from four sites across the tropical Pacific Ocean for the time period spanning 2012–2016 (Figure 1). We compare these new data to previous data, where available, to test the null hypothesis that the $\delta^{18}O_{sw}$-salinity relationship is uniform at each site and constant across space and time. We then assess the $\delta^{18}O_{sw}$-salinity relationship in isotope-enabled model simulations. Finally, we draw conclusions about broad patterns in the $\delta^{18}O_{sw}$-salinity relationship across the tropical Pacific in observations and model simulations and discuss possible causes of these variable relationships.

2. Study Sites and Methods

2.1. Sites

Seawater samples were collected from four locations (Figures 1 and 2): Manus, Papua New Guinea (2.06°S 147.43°E), Koror, Palau (7.32°N 134.46°E), Kiritimati, Republic of Kiribati (2.00°N, 157.48°W), and Santa Cruz Island, Galápagos, Ecuador (0.74°S 90.30°W). At each site, seawater samples were taken from the same location weekly for both salinity and stable isotope analysis between 2012 and 2016. Sites for sample collection were selected away from visible surface runoff and were based on preliminary field measurements that indicated nearshore salinities similar to those measured farther away from shore, suggesting limited groundwater flux. Water was taken from 0.5–1.0 m below the surface to avoid freshwater films. We also sampled seawaters spatially to assess salinity and $\delta^{18}O_{sw}$ values. At Manus, samples were taken from accessible shorelines of the island over the course of a week in April–May 2013. Kiritimati samples were taken from the coastline of the island (from shore and from a boat) during 2 week field excursions in May 2012

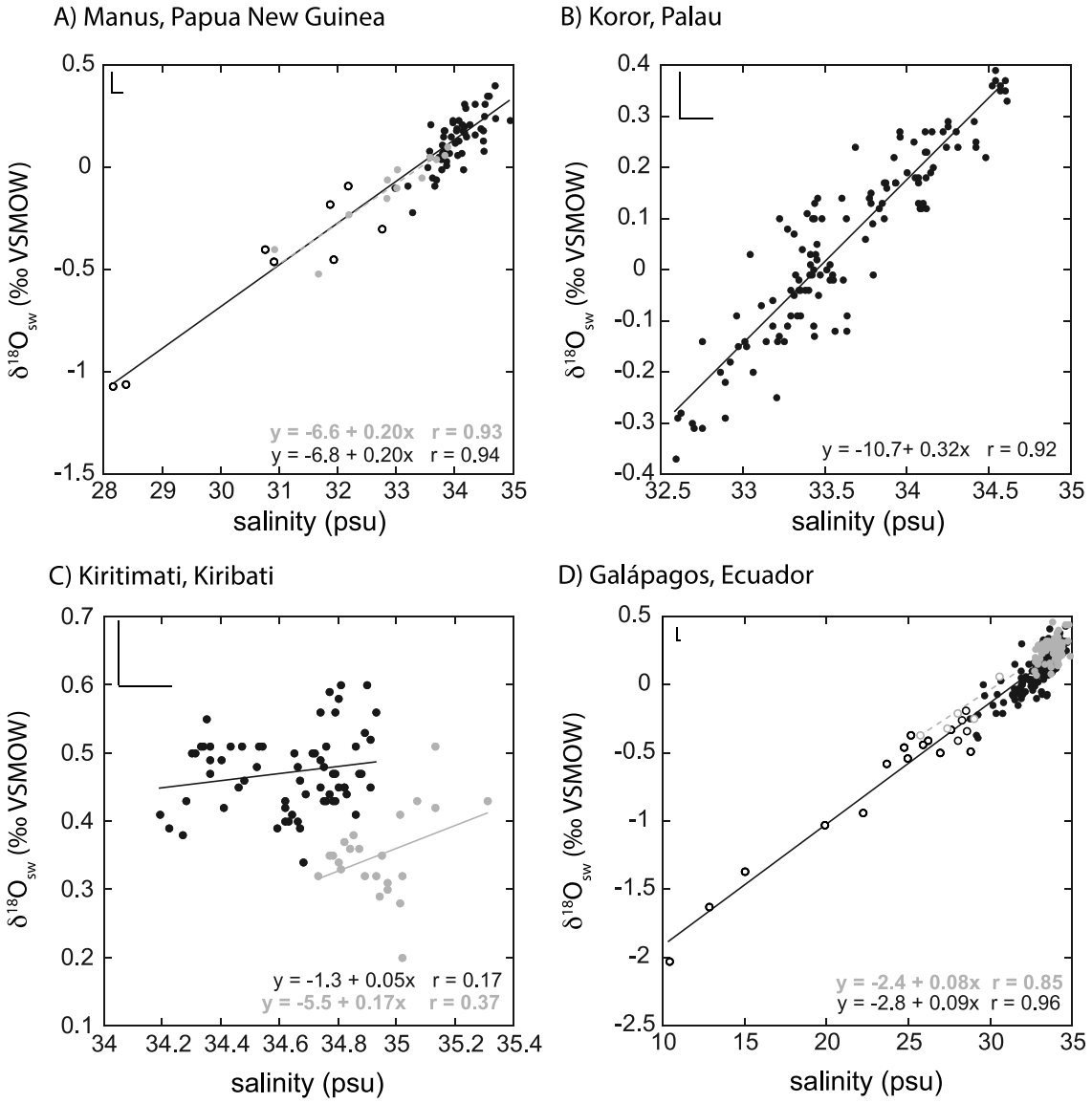

Figure 2. Scatterplots of temporal (black circles) and spatial (gray circles) $\delta^{18}O_{sw}$ and salinity values for (a) Manus, (b) Palau, (c) Kiritimati, and (d) Galápagos. Open (versus filled) circles are statistical outliers, likely indicative of local freshwater runoff or evaporation. Upper left of each plot denotes uncertainty in $\delta^{18}O_{sw}$ and salinity. Confidence intervals and r^2 values shown in Table 1. Coefficients for $\delta^{18}O_{sw}$ and salinity relationships without outliers are presented in Table S1.

and August 2013. In the Galápagos, samples were taken during 2 week field excursions in October 2012 and January 2015 from across the archipelago by boat and from shore. Seawater samples used for salinity measurements were collected in 60 ml amber glass bottles rinsed 3 times with the sampled seawater, capped and sealed with parafilm. Seawater samples used for stable isotope measurements were taken simultaneously with the samples for salinity and stored in 3.5 ml glass crimp-top vials. After shipment to the University of Illinois Urbana–Champaign or Georgia Institute of Technology, samples were stored, refrigerated, in the dark, prior to analysis.

Seawater samples were measured on a Picarro L2120-*i* water isotope analyzer at the University of Illinois Urbana–Champaign. Reported data were calibrated with National Institute of Standards and Technology Vienna Standard Mean Ocean Water 2 (VSMOW2), Greenland Ice Sheet Project (GISP), and Standard Light Antarctic Precipitation 2 (SLAP2) standards and three internal lab standards ($\delta^{18}O$ = −10.2, −6.8, 0.3‰, δD −72.3‰, −41.9‰, 0.9‰). Total measurement error, determined from analyses of known liquid standards,

Table 1. Sample Size, Mean $\delta^{18}O_{sw}$ and Salinity (1σ), Slope and Intercept With 95% Confidence Intervals, r^2 Values, and Root-Mean-Square Error Using Studentized Residuals for Temporal and Spatial $\delta^{18}O_{sw}$ and Salinity From Each Site[a]

Site Name	N	Mean $\delta^{18}O_{sw}$	Mean Salinity	Slope	Intercept	r^2	RMSE
Manus temporal	62	0.05 ± 0.28	33.6 ± 1.3	0.20 ± 0.02	−6.8 ± 0.6	**0.89**	1.025
Manus spatial	12	−0.10 ± 0.19	32.9 ± 0.9	0.20 ± 0.05	−6.6 ± 1.8	**0.87**	1.863
Palau temporal 2013–2016	123	0.05 ± 0.18	33.6 ± 0.5	0.32 ± 0.02	−10.7 ± 0.8	**0.85**	1.017
Palau temporal 1998–2000	56	0.09 ± 0.25	33.8 ± 0.6	0.42 ± 0.03	−14.2 ± 1.0	**0.94**	1.045
Kiritimati temporal	65	0.47 ± 0.06	34.6 ± 0.2	0.05 ± 0.07	−1.3 ± 2.4	0.03	1.028
Kiritimati spatial	23	0.35 ± 0.06	34.9 ± 0.1	0.17 ± 0.19	−5.5 ± 6.7	0.14	1.161
Galápagos temporal	173	0.04 ± 0.33	32.0 ± 3.5	0.09 ± 0.01	−2.8 ± 0.1	**0.92**	1.014
Galápagos spatial	93	0.23 ± 0.10	33.6 ± 1.3	0.08 ± 0.01	−2.4 ± 0.4	**0.72**	1.020

[a]Bold r^2 values are significant at the 95% confidence level.

is <0.1‰ for $\delta^{18}O$ and <0.8‰ for δD. Memory and drift corrections were applied using the internal standards listed above [*van Geldern and Barth*, 2012]. Data are reported in δ notation (‰), relative to VSMOW. Salinity was measured on a Thermo Scientific Orion Star A212 benchtop conductivity meter, calibrated every 10 samples using 50.0 mS/cm certified conductivity solution. Twenty milliliter aliquots of seawater samples were measured 5 times while maintaining a constant sample temperature of 25.0°C in a dry bead heat block. Salinity values are reported as the average of the five measurements. Values are reported as practical salinity units (psu). Instrument measurement resolution is 0.01 psu. Measured standard deviations for individual samples are <0.1 psu and duplicate measurements on samples indicate a mean absolute difference of 0.1 psu.

We also assess previously published $\delta^{18}O_{sw}$ and salinity data. These data were downloaded from the Goddard Institute of Space Studies (GISS) seawater isotope database (http://data.giss.nasa.gov/o18data/) and include data measured biweekly at Koror, Palau, from 1998 to 2000 [*Morimoto et al*., 2002] and monthly data at three Galápagos sites from 1993 to 1994 [*Wellington et al*., 1996]. Spatial data sets of $\delta^{18}O_{sw}$ and salinity from north of the Galápagos and the Panama Bight region [*Benway and Mix*, 2004], and north of Kiritimati along the Line Islands Ridge [*Conroy et al*., 2014] are also assessed relative to the new data presented here. We also compare site salinity data with NASA Aquarius sea surface salinity estimates [*Lee et al*., 2012], using 7 day running mean salinity (version 4.0) for the grid cells closest to the latitude and longitude of the sites during the time period of overlap. Daily precipitation in mm/d is taken from stations at Santa Cruz, Galápagos, Cassidy Airport, Kiritimati, and Koror, Palau. For Manus, station precipitation data were not available for the entire period, so Tropical Rainfall Measuring Mission (TRMM) 3B42 v7 daily data were used for the 0.25° by 0.25° grid representing the island [*Huffman et al*., 2007]. Evaporation values used (shown in mm/d) are from the daily, gridded 1° by 1° OAFlux ocean evaporation data set [*Yu and Weller*, 2007]. Zonal and meridional currents (m/s) for the grid cells representing each site are taken from the Ocean Surface Current Analysis-Real time database [*Bonjean and Lagerloef*, 2002]. Daily resolved SST is from the NOAA optimum interpolation 1/4° daily SST blended with Advanced Very High Resolution Radiometer (AVHRR) SST data set [*Reynolds et al*., 2007]. For assessment of correlations between monthly averaged $\delta^{18}O_{sw}$ and regional, gridded salinity, precipitation, and evaporation, we use Argo mixed layer salinity [*Argo*, 2000], Global Precipitation Climatology Project v2.3 (GPCP2.3) precipitation [*Adler et al*., 2003], and monthly WHOI OAflux evaporation [*Yu and Weller*, 2007]. We also compare the observed $\delta^{18}O_{sw}$-salinity relationships with temporal $\delta^{18}O_{sw}$-salinity relationships from a 100 year long, isotope-enabled control simulation (1850 conditions) of the GISS ModelE-R, ("CMIP5 version") reported in *Thompson et al*. [2013]. The simulated $\delta^{18}O_{sw}$-salinity relationship was assessed from monthly average salinity and $\delta^{18}O_{sw}$ in the 1° × 1° grid box nearest to each site over the 100 year period.

3. Results

3.1. Manus

Sixty-two samples collected from Manus between 27 April 2013 and 9 July 2014 have a mean $\delta^{18}O_{sw}$ value of 0.05 ± 0.28‰ (1σ) and a mean salinity value of 33.6 ± 1.3 psu (1σ). A strong linear relationship was present between these two variables (Table 1), with a slope of 0.20 ± 0.02 ‰/psu and an intercept of −6.8 ± 0.6‰

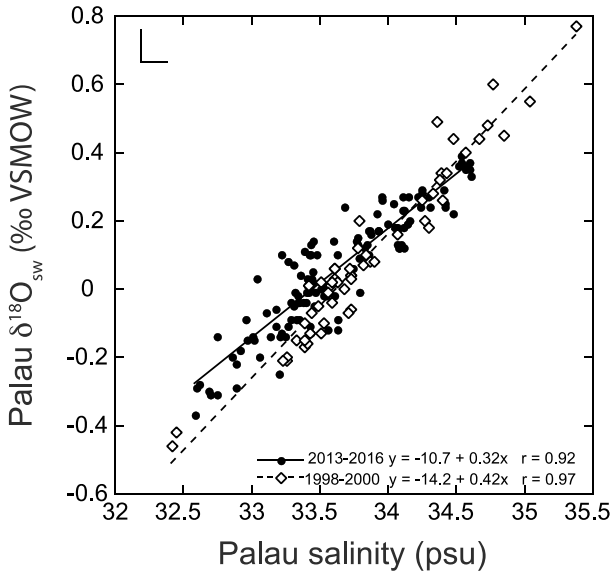

Figure 3. Scatterplot of temporal $\delta^{18}O_{sw}$ and salinity from Palau, with previously published temporal $\delta^{18}O_{sw}$ and salinity data from 1998 to 2000. Filled circles and solid line represent data presented in this manuscript, open diamonds and dashed line indicate data from *Morimoto et al.* [2002].

(Figure 2a). The Manus spatial data set comprises 14 samples from along the island's coastline collected from 27 April to 7 May 2013, which also display a strong linear relationship (Table 1). Two spatial data points were removed prior to analysis: one was contaminated by rain, as it was collected during a precipitation event, and one sample from Seadler Harbor, adjacent to the largest town on the island, was influenced by human runoff. The slope (0.20 ± 0.05‰/psu) and intercept (−6.6 ± 1.8‰) from the spatial data set overlap the slope and intercept values (within 1σ) calculated with the temporal data set.

3.2. Palau

One hundred twenty-three samples south of Koror, Palau, collected between 7 February 2013 and 24 April 2016, have a mean $\delta^{18}O_{sw}$ value of 0.05 ± 0.18‰ and a mean salinity value of 33.6 ± 0.5 psu. A strong linear relationship was present between these two variables (Table 1), with a slope of 0.32 ± 0.02‰/psu and an intercept of −10.7 ± 0.8‰ (Figure 2b). At the same location, from 1998 to 2000, mean $\delta^{18}O_{sw}$ was 0.09 ± 0.25‰ and mean salinity was 33.8 ± 0.6 psu [*Morimoto et al.*, 2002]. The 1998–2000 data set contains $\delta^{18}O_{sw}$ and salinity values higher than those measured recently (Figure 3), but the 2013–2016 data do overlap the 1998–2000 data. However, the earlier data from 1998 to 2000 have a significantly higher slope (0.42 ± 0.03‰/psu) and lower intercept (−14.2 ± 1.0‰).

3.3. Kiritimati

Sixty-five samples collected weekly from Kiritimati between 20 August 2013 and 31 December 2014 have a mean $\delta^{18}O_{sw}$ value of 0.47 ± 0.06‰ and a mean salinity value of 34.6 ± 0.2 psu. The overall range of $\delta^{18}O_{sw}$ and salinity values represented by these samples is small relative to the measurement uncertainty, and we find insignificant relationships between these two variables. A data set of spatial $\delta^{18}O_{sw}$ and salinity values from May 2012 to August 2013 also indicates a weak relationship between $\delta^{18}O_{sw}$ and salinity, with a slope of 0.17 ± 0.19‰/psu and intercept of −5.5 ± 6.7‰ (Table 1 and Figure 2c).

3.4. Galápagos

We measured 173 paired seawater samples for $\delta^{18}O_{sw}$ and salinity collected from the southeastern coast of Santa Cruz Island, Galápagos, between 8 October 2012 and 25 April 2016. Mean $\delta^{18}O_{sw}$ was 0.04 ± 0.33‰ and mean salinity was 32.0 ± 3.5 psu. A significant linear relationship was present between these two variables (Table 1 and Figure 2d). Spatially, we collected 93 surface seawater samples from across the archipelago during October 2012 and January 2015 (Table 1 and Figure 2d). The slope and intercept from the spatial data set (0.08 ± 0.01‰/psu, −2.4 ± 0.4‰) and the temporal data set (0.09 ± 0.01‰/psu, −2.8 ± 0.1‰) overlap within 1σ. The $\delta^{18}O_{sw}$ data from 1993 to 1994 taken from three sites (Urvina Bay, Bartolomé, and Champión) across the archipelago range from 0.05 to 0.52‰, with a mean value of 0.28 ± 0.12‰ [*Wellington et al.*, 1996], falling within the range of our measurements. Although paired salinity values for these $\delta^{18}O_{sw}$ values are not reported on the GISS database, *Wellington et al.* [1996] found a significant $\delta^{18}O_{sw}$-salinity relationship at only one of the three sites, Bartolomé Island. The slope and intercept of this relationship were not reported.

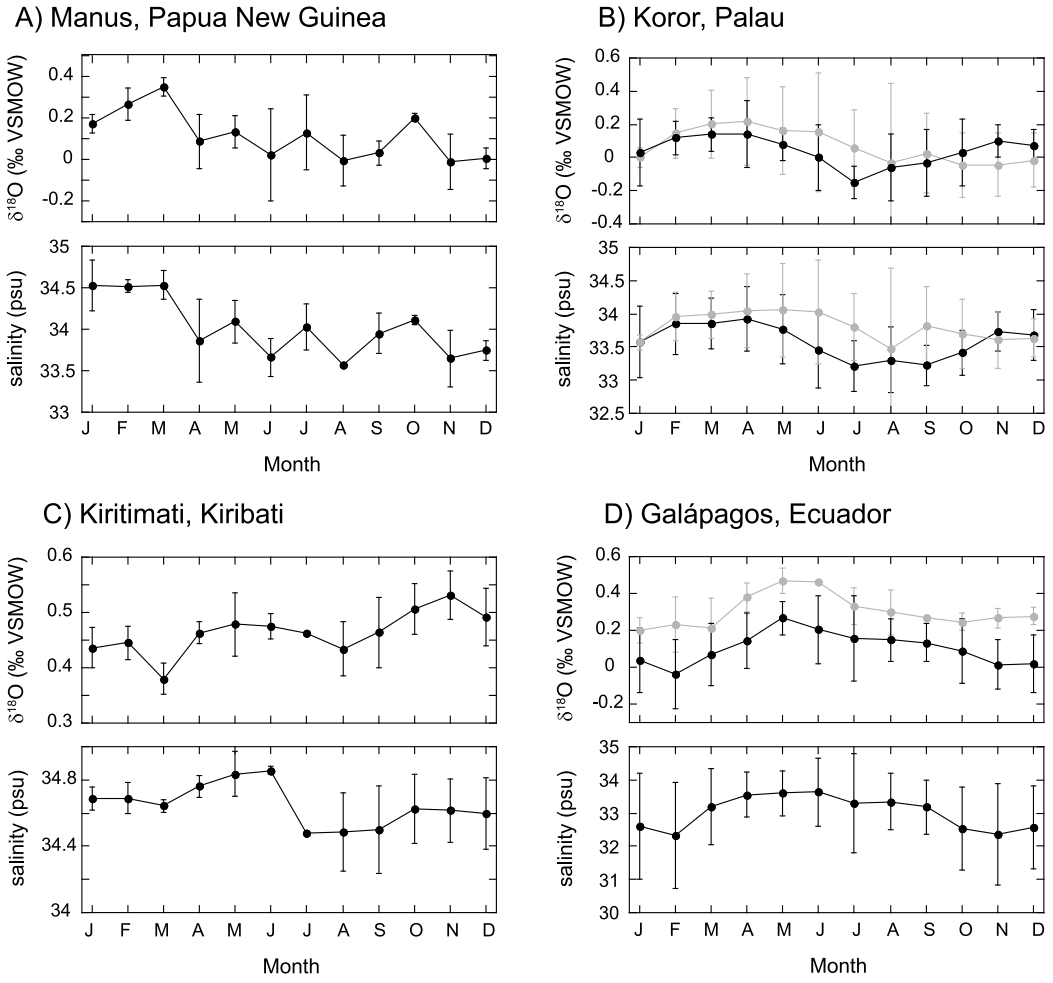

Figure 4. Mean monthly (and 1σ) $\delta^{18}O_{sw}$ and salinity values for each site: (a) Papua New Guinea; (b) Palau, gray circles and line represent previous $\delta^{18}O_{sw}$ and salinity from *Morimoto et al.* [2002]; (c) Kiritimati; and (d) Galápagos. Gray circles and line indicate previous $\delta^{18}O_{sw}$ data spanning 1993–1994 from *Wellington et al.* [1996].

3.5. Consideration of Low $\delta^{18}O_{sw}$ and Salinity Values

Measured salinity at each site is consistently fresher than satellite-estimated sea surface salinity, with the exception of the Galápagos, where values are similar, although the timing of seasonal variability is often similar in both data sets (Figures S2–S5 in the supporting information). More saline, remotely sensed values are not surprising, as satellite data reflect 1° × 1° areas of open ocean, whereas we record variability at a finer spatial scale closer to shore. Thus, in this particular study, satellite data are not useful for assessing local $\delta^{18}O_{sw}$-salinity relationships. Within our data sets, some measurements are fresher or more saline than typical open-ocean sea surface salinity values. We consider such data in two ways. First, we excluded points in our spatial data sets that were clearly influenced by human-induced freshening (i.e., wastewater near towns/ports), were sampled in environments isolated from the open ocean (i.e., within Kiritimati lagoon), or, in the case of one Manus spatial sample, were sampled during a large rain storm (sample was contaminated by rain). However, we keep values that are fresher than local mean seawater and are likely a result of natural runoff or groundwater flux. Second, to assess how $\delta^{18}O_{sw}$-salinity relationships are influenced by fresher/lower $\delta^{18}O_{sw}$ values, we calculate the $\delta^{18}O_{sw}$-salinity relationship excluding outlier values, defined as values less (greater) than the lower (upper) quartile minus (plus) 1.5 times the interquartile distance (upper minus lower quartile) for each data set, shown in Figure S1 and reported in Table S2. The resulting slopes and intercepts are not significantly different for the Manus temporal data set (see Table S1 for comparison). The Palau data set had no outliers defined in this manner. The spatial Kiritimati slope

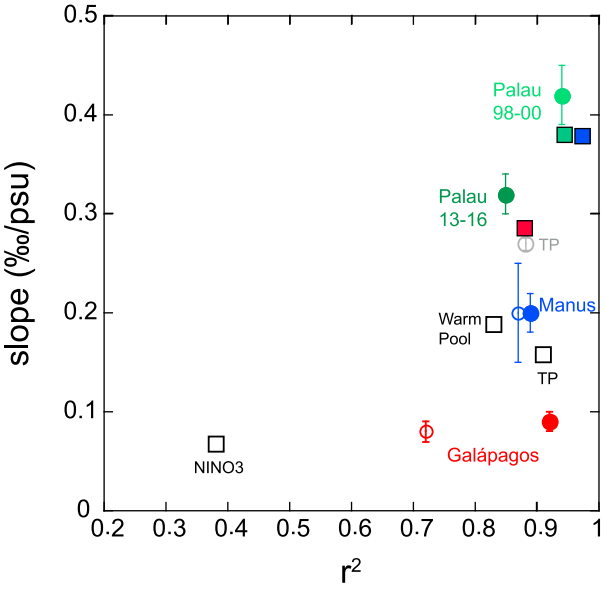

Figure 5. Slope and r^2 values for each site. Filled circles indicate temporal data, open circles indicate spatial data. Open gray circle represents tropical Pacific values from *LeGrande and Schmidt* [2006]. Squares indicate results from isotope-enabled model simulations. Black open squares are spatial NINO3, west Pacific warm pool and tropical Pacific basin average values from isotope-enabled HadCM3 [*Russon et al.*, 2013]. Colored, filled squares represent temporal (monthly) data for grids representing each site from GISS Model E2.

and intercept remained statistically insignificant. The Galápagos spatial and temporal slopes and intercepts are not significantly different when outliers are removed, although the spatial relationship weakens, as we do not capture a substantial range of values relative to measurement uncertainty when outliers are removed.

3.6. Mean Monthly $\delta^{18}O_{sw}$ and Salinity

Monthly climatologies of $\delta^{18}O_{sw}$ and salinity show the seasonal cycle in the data at each site, as well as interannual variability at Palau and Galápagos, where previous data are available (Figure 4). At Manus, $\delta^{18}O_{sw}$ and salinity are highest in January, February, and March. Mean monthly $\delta^{18}O_{sw}$ and salinity are strongly correlated, with a slope and intercept similar to that obtained using weekly data (Figure S6). At Palau, $\delta^{18}O_{sw}$ and salinity values are highest from November to May. Previous data [*Morimoto et al.*, 2002] show similar seasonality in $\delta^{18}O_{sw}$ and salinity, but $\delta^{18}O_{sw}$ and salinity decrease later in the calendar year (Figure 4b). The slope and intercept values for mean monthly Palau data (Figure S6) are similar to the slopes and intercepts calculated using weekly/biweekly data. As there is limited variability in the shorter Kiritimati data set, there is not a significant relationship between the two variables on the mean monthly time scale (Figure S6). $\delta^{18}O_{sw}$ and salinity are highest in the Galápagos from April to June, decrease from July to January, and are lowest in November through March. The slope is higher and the intercept is lower in the mean monthly data, in comparison to slope and intercept of the weekly data (Figure S6). Previous $\delta^{18}O_{sw}$ values averaged into mean monthly values from three sites across the Galápagos archipelago from 1993 to 1994 [*Wellington et al.*, 1996] show a similar seasonal pattern, although $\delta^{18}O_{sw}$ is lowest beginning in January and extending to March, and values are 0.14 to 0.27‰ higher.

4. Discussion

4.1. $\delta^{18}O_{sw}$-Salinity Relationships Across the Tropical Pacific

Assessment of the $\delta^{18}O_{sw}$-salinity relationship at four different sites reveals distinct slope and intercept values, with higher slopes and lower intercepts in the western tropical Pacific sites (Palau and Manus) relative to the eastern tropical Pacific site (Galápagos) (Figure 5). The central tropical Pacific (Kiritimati) $\delta^{18}O_{sw}$-salinity relationships are insignificant, due to the limited variance in the data set. At Manus, Palau, and Galápagos, the $\delta^{18}O_{sw}$-salinity slopes are all significantly different from the mean tropical Pacific $\delta^{18}O_{sw}$-salinity slope of 0.27 ‰/psu (t values = 6.10, 3.73, and 29.75, DF = 344, 405, 455, $p < 0.01$ for Manus, Palau, and Galápagos, respectively).

At Manus and Galápagos, where we sampled spatially as well as temporally, spatial $\delta^{18}O_{sw}$-salinity relationships are not significantly different from the temporal $\delta^{18}O_{sw}$-salinity relationships (t = 0.28, 1.82, DF = 262, 70, p = 0.78, 0.07, for Manus and Galápagos respectively). The similarity of the spatial and temporal relationships suggests potentially similar controls on the $\delta^{18}O_{sw}$-salinity relationship in both space and time. For

example, seawater at different sampling locations may contain different contributions from specific water masses, runoff, precipitation, or precipitation sources with varying $\delta^{18}O_p$; varying advection, precipitation rates, and precipitation sources or types may also shape the temporal $\delta^{18}O_{sw}$-salinity relationship.

At Kiritimati, the spatial and the temporal relationships are insignificant. However, previous spatial data encompassing a larger meridional gradient of ~20°, between Hawaii and the Line Islands, show a significant relationship with a slope of 0.23‰/psu from data available in the GISS $\delta^{18}O_{sw}$ database and 0.31‰/psu from samples taken during May 2012 [*Conroy et al*., 2014]. Previous spatial data also show that, zonally, across the boundary between the more saline central tropical Pacific and fresher western tropical Pacific, the slope of the $\delta^{18}O_{sw}$-salinity relationship approximates the pantropical Pacific slope of 0.27‰/psu [*Fairbanks et al*., 1997]. Thus, a longer or spatially larger Kiritimati data set capturing a wider range of $\delta^{18}O_{sw}$ and salinity values may ultimately produce a significant $\delta^{18}O_{sw}$-salinity relationship for this site.

At the Palau site, the $\delta^{18}O_{sw}$-salinity relationship varies temporally. Paired $\delta^{18}O_{sw}$ and salinity measurements taken biweekly in Palau from 1998 to 2000 indicate a difference in the relationship between these two variables relative to our data from 2013 to 2016. Although our new data overlap the range of previous data taken by *Morimoto et al.* [2002], data from 1998 to 2000 have a significantly higher slope and lower intercept ($t = 5.41$, DF = 175, $p < 0.01$). The two sampling intervals at Palau each captured one extreme of ENSO: the end of a strong El Niño event and a strong La Niña event occurred in the 1998–2000 sampling interval, and a strong El Niño event occurred during the 2013–2016 sampling interval. A higher slope during the period containing a strong La Niña event may be due to a greater degree of atmospheric organization in the western tropical Pacific at this time, producing precipitation with a lower $\delta^{18}O$ value, which would increase the per mil change in surface seawater per unit change in psu. Yet overall, the 1998–2000 samples have higher salinity and $\delta^{18}O_{sw}$ values, suggesting other factors, such as changes in ocean circulation, may be more influential on the $\delta^{18}O_{sw}$-salinity relationship.

Additional $\delta^{18}O_{sw}$ and salinity data are also available from Galápagos, permitting a deeper investigation into the stability of the $\delta^{18}O_{sw}$-salinity relationship in the eastern tropical Pacific. A weak relationship between $\delta^{18}O_{sw}$ and salinity was noted when considering mean monthly data from 1993 to 1994 [*Wellington et al*., 1996], whereas we find a significant relationship between $\delta^{18}O_{sw}$ and salinity at Puerto Ayora on both the weekly and mean monthly time scale from 2013 to 2016 (Figures 2d and S6). This relationship remains significant when we exclude fresh outliers (Figure S1). A strong relationship has also been found in spatial $\delta^{18}O_{sw}$ and salinity data north of the Galápagos to the Panama Bight region [*Benway and Mix*, 2004]. *Benway and Mix* [2004] found that mixed layer $\delta^{18}O_{sw}$ and sea surface salinity in this region were defined by multiple linear relationships, with reported slopes ranging from 0.07 to 0.25‰/psu and intercepts from −8.5 to −2.5‰. Here higher slopes and lower intercepts indicate the influence of remote moisture transported across the Panama isthmus, and lower slopes and higher intercepts are hypothesized to be due to local freshwater forcing [*Benway and Mix*, 2004]. At the Galápagos site, the relatively low slope and high intercept from the 2012–2016 data set are similar to one *Benway and Mix* [2004] relationship, derived from a transect of samples at 95°W, 5.6–11°N, which have a slope of 0.07‰/psu and intercept of −2.5‰. A similar relationship in the Galápagos suggests that the influence of remote, depleted vapor sources from the Caribbean is reduced southwest of the Panama Bight.

4.2. $\delta^{18}O_{sw}$-Salinity Relationship in Isotope-Enabled Model Simulations

Isotope-enabled ocean models and coupled ocean-atmosphere models are essential tools for investigating the stability of the $\delta^{18}O_{sw}$-salinity relationship across space and time. Recent model results have questioned the assumption of constant $\delta^{18}O_{sw}$-salinity relationships across water masses and ocean basins with different background climates: Simulated $\delta^{18}O_{sw}$-salinity slopes derived from the isotope-enabled Hadley Centre Model 3 (HadCM3) [*Holloway et al*., 2016] and Goddard Institute for Space Studies (GISS) ModelE-R [*LeGrande and Schmidt*, 2011] vary under different boundary conditions as well as spatially versus temporally. Although *Holloway et al.* [2016] infer that the $\delta^{18}O_{sw}$-salinity relationship is relatively more robust across space and time in the tropical Pacific relative to other ocean regions, *Russon et al.* [2013] used a 750 year preindustrial control simulation of the isotope-enabled HadCM3 to show that the $\delta^{18}O_{sw}$-salinity relationship differs between the NINO3, west Pacific warm pool and western cold tongue regions. On finer spatial scales, isotope-enabled regional ocean models provide insight into the controls on local $\delta^{18}O_{sw}$-salinity

relationships. For example, a regional isotope-enabled ocean model of the Line Islands shows a weak modern relationship between $\delta^{18}O_{sw}$ and salinity around Kiritimati [*Stevenson et al.*, 2015]. This downscaled experiment highlighted the role of mesoscale eddies in local $\delta^{18}O_{sw}$ budgets, and the potential for large spatial variations in $\delta^{18}O_{sw}$ and salinity across the Line Islands [*Stevenson et al.*, 2015].

Although simulated $\delta^{18}O_{sw}$-salinity slopes do not agree in magnitude with observed slopes, the spatial $\delta^{18}O_{sw}$-salinity slopes calculated by *Russon et al.* [2013] reveal a higher slope to the west, in the warm pool region, and a lower slope in the eastern tropical Pacific NINO3 region, similar to our observations. We find the same pattern in the temporal, monthly $\delta^{18}O_{sw}$-salinity relationships from GISS Model-E2, with the highest slopes found for grid cells representing Palau and Manus and the lowest for the Galápagos (Figure 5). Given the diversity of data sources in Figure 5, the strength (r^2) and slopes of the simulated $\delta^{18}O_{sw}$-salinity relationships would be expected to vary. Yet the consistently higher slopes in the western tropical Pacific suggest a similar driver in both models and observations. We hypothesize that this is the stronger hydrologic cycle and greater variability in $\delta^{18}O_p$ in the western tropical Pacific. A more detailed assessment of controls on $\delta^{18}O_{sw}$ and salinity across the tropical Pacific is provided in the subsequent section.

4.3. Drivers of Variability in Tropical Pacific $\delta^{18}O_{sw}$-Salinity Relationships

$\delta^{18}O_{sw}$ and salinity values for a given water mass are dependent upon regional precipitation, evaporation, runoff, advection, upwelling, and diffusion. The relationship between $\delta^{18}O_{sw}$ and salinity may vary spatially and temporally as a consequence of changes in the $\delta^{18}O$ value of precipitation or runoff, as well as the contributions of different water masses to a given region. Precipitation or runoff with a lower $\delta^{18}O$ value will produce a higher $\delta^{18}O_{sw}$-salinity slope and lower intercept, or "freshwater endmember," which reflects $\delta^{18}O$ when salinity equals zero [*Delaygue et al.*, 2001]. Evaporation also influences the $\delta^{18}O_{sw}$-salinity intercept and can depress the $\delta^{18}O_{sw}$-salinity slope [*Conroy et al.*, 2014; *Delaygue et al.*, 2001]. In addition, variability in advection and upwelling rates of water masses that formed in different regions can shape the mixed layer $\delta^{18}O_{sw}$-salinity relationship for a given locale, especially in areas of complex circulation [*Benway and Mix*, 2004]. Associations between SST and $\delta^{18}O_{sw}$ are also important to assess, as SST can delineate changing atmospheric and oceanic conditions that may shape the $\delta^{18}O_{sw}$-salinity relationship (e.g., ENSO, upwelling), and covariance of SST and $\delta^{18}O_{sw}$ can confound SST-based interpretations of $\delta^{18}O$ values of fossil corals [*Russon et al.*, 2013]. In this section we consider the potential roles for these factors at each site based on the $\delta^{18}O_{sw}$-salinity intercepts, $\delta^{18}O$ values of precipitation, and correlations between time series of $\delta^{18}O_{sw}$, precipitation, evaporation, SST, and zonal (*U*) and meridional (*V*) currents at each site.

First, we consider the overarching observed pattern of higher slopes and lower intercepts in the western tropical Pacific relative to the eastern tropical Pacific. Isotopic distillation and subsequently lower $\delta^{18}O$ values of precipitation ($\delta^{18}O_p$) accompanying transport of vapor from the tropics to the extratropics is the key factor driving higher $\delta^{18}O_{sw}$-salinity slopes in extratropical water masses [*LeGrande and Schmidt*, 2011]. In a similar fashion, a stronger hydrologic cycle and greater atmospheric convergence over the western tropical Pacific is associated with lower $\delta^{18}O_p$ relative to the central and eastern tropical Pacific [*Conroy et al.*, 2013]. Thus, greater precipitation rates and lower $\delta^{18}O_p$ in the western tropical Pacific may set the higher slope and lower intercepts found in Manus and Palau relative to the Galápagos.

The $\delta^{18}O_{sw}$-salinity intercept at Manus (−6.8‰) is lower than mean annual amount weighted $\delta^{18}O_p$ from nearby GNIP sites of Jayapura (mean $\delta^{18}O_p = -5.7$‰) and Madang (mean $\delta^{18}O_p = -4.8$‰) but falls well within the range of measured $\delta^{18}O_p$ for the region, where recent measurements of rainfall events show storms with $\delta^{18}O$ values as low as −14.0‰ [*Conroy et al.*, 2016]. Temporally, Manus $\delta^{18}O_{sw}$ is negatively correlated with local evaporation and SST and negatively correlated with precipitation (Table 2). These correlations suggest that warmer SST drives both enhanced evaporation at the surface but also leads to enhanced convection and precipitation, which ultimately lowers $\delta^{18}O_{sw}$. Manus $\delta^{18}O_{sw}$ is also positively correlated with *U*, with higher $\delta^{18}O_{sw}$ coinciding with increased westerly (eastward) flow (Table 2 and Figure S2). The New Guinea Coastal Current passes south of Manus [*Fine et al.*, 1994; *Kuroda*, 2000]. This current changes direction seasonally and may influence $\delta^{18}O_{sw}$ at Manus. During boreal winter, when $\delta^{18}O_{sw}$ is highest and westerly flow is strongest, the NGCC is northwesterly. It is unclear why this current would transport high $\delta^{18}O_{sw}$ water, but it is associated with increased upwelling south of the equator [*Kuroda*, 2000], which may attenuate the role of freshwater fluxes in decreasing $\delta^{18}O_{sw}$ locally.

Table 2. Correlation Coefficients Between Monthly Averaged Site $\delta^{18}O_{sw}$ and Local (Site) Salinity, Precipitation, Evaporation, SST, Zonal, and Meridional Currents Plotted in Figures S2–S5[a]

Site	Site Salinity	P	E	SST	U	V
Manus $\delta^{18}O_{sw}$	**0.87**	*−0.49*	*−0.51*	**−0.62**	**0.66**	0.40
Palau $\delta^{18}O_{sw}$ (2013–2016)	**0.93**	**−0.57**	**−0.53**	**−0.51**	*−0.33*	−0.13
Palau detrended	**0.82**	**−0.52**	**−0.61**	−0.22	−0.11	**0.43**
Kiritimati $\delta^{18}O_{sw}$	0.29*	−0.42*	0.21	0.31	0.05	0.21
Galápagos $\delta^{18}O_{sw}$	**0.84**	−0.07*	−0.17	−0.03	*−0.29*	*0.26*

[a]These daily data were converted to monthly averages prior to correlation. Bold values are significant at the 95% confidence level. Italicized values significant at the 90% confidence level. Significance is computed with effective sample size to account for serial correlation [*Dawdy and Matalas*, 1964]. Asterisks indicate nonnormal data distribution (computed using Lilliefor's test) and the use of Spearman's rho to assess relationship strength, rather than Pearson's R. We also report correlation coefficients for detrended data from Palau, as Palau $\delta^{18}O_{sw}$ and salinity possess a linear trend over the time period investigated.

At Palau, freshwater fluxes also play a strong role in shaping the temporal $\delta^{18}O_{sw}$-salinity relationship. $\delta^{18}O_{sw}$ is negatively correlated with precipitation, evaporation, and SST (Table 2 and Figure S3). Yet here the observed intercepts are much lower than mean annual, amount weighted $\delta^{18}O_p$ value of −4.5‰. One point of consideration is an oversized role for rare, large, low $\delta^{18}O_p$ events (i.e., typhoons, MJO events) in shaping the overall $\delta^{18}O_{sw}$-salinity relationship, as *Benway and Mix* [2004] hypothesized for the Panama Bight. Another possibility is that the water mass represented by the $\delta^{18}O_{sw}$-salinity relationship at Palau is of North Pacific origin, as North Pacific water is defined by a higher $\delta^{18}O_{sw}$-salinity slope of 0.44‰/psu and lower intercept of −15.13‰ relative to the tropical Pacific [*Legrande and Schmidt*, 2006]. An additional consideration is the role of upwelled water [*Wolanski et al*., 2004] in shaping the surface $\delta^{18}O_{sw}$-salinity relationship at the Palau site. Subsurface water masses have distinct slopes and intercepts relative to surface waters, depending on their geographical origin [*LeGrande and Schmidt*, 2006]. For example, subsurface waters in the eastern (41–400 m depth) and central (80–500 m depth) Pacific have higher slopes and lower intercept values than surface waters [*Benway and Mix*, 2004; *Conroy et al*., 2014] similar to the high slope and low intercept of the Palau $\delta^{18}O_{sw}$-salinity data set. However, more paired subsurface $\delta^{18}O_{sw}$ and salinity measurements are required to test this hypothesis.

Kiritimati $\delta^{18}O_{sw}$ variability is low and sample size is small, so a strong relationship with ocean and atmospheric variables was not expected. There is a shift to lower salinity values in August 2014 in both the satellite and site salinity measurements (Figure S4). Additionally, at this time there is a transition from weak westerly flow to stronger easterly flow. However, $\delta^{18}O_{sw}$ remains relatively consistent during this transition. At Kiritimati, mesoscale tropical instability waves, or eddies, may play a key role in controlling local $\delta^{18}O_{sw}$, salinity, and the relationship between the two variables [*Stevenson et al*., 2015]. Surface current data that resolve such small-scale circulation features are required to thoroughly investigate a correlation between $\delta^{18}O_{sw}$ and ocean circulation in this region.

Overall, the observed Galápagos intercept (−3.3‰) is similar to mean annual amount weighted precipitation for the region (−2.8‰). Hence, it appears that here local precipitation defines the $\delta^{18}O_{sw}$-salinity slope and intercept. The $\delta^{18}O_{sw}$-salinity relationship in the Galápagos reported here is similar to one of several "secondary" $\delta^{18}O_{sw}$-salinity relationships observed west of the Panama Bight along a transect north of the Galápagos (5.7–11°N, 95°W) [*Benway and Mix*, 2004]. This relationship was interpreted to reflect local, rather than remote precipitation as a main driver of the $\delta^{18}O_{sw}$-salinity relationship. Detection of this relationship farther south suggests that regional $\delta^{18}O_{sw}$-salinity relationships may migrate. However, considering correlation coefficients between Galápagos $\delta^{18}O_{sw}$ and other variables, the only significant relationships detected are between *U*, *V*, and $\delta^{18}O_{sw}$ (Table 2 and Figure S5). Hence, advection appears to have a stronger influence on $\delta^{18}O_{sw}$ here relative to freshwater fluxes.

Spatial correlation maps of site $\delta^{18}O_{sw}$ and gridded ocean and climate variables offer a means to explore if local $\delta^{18}O_{sw}$ is representative of regional ocean and atmosphere variability. Here we correlate the two longest, monthly averaged $\delta^{18}O_{sw}$ time series from Galápagos and Palau, which span similar time periods, to investigate how $\delta^{18}O_{sw}$ at these sites is related to regional sea surface salinity, precipitation, and evaporation in 20° × 20° areas surrounding each island collection site.

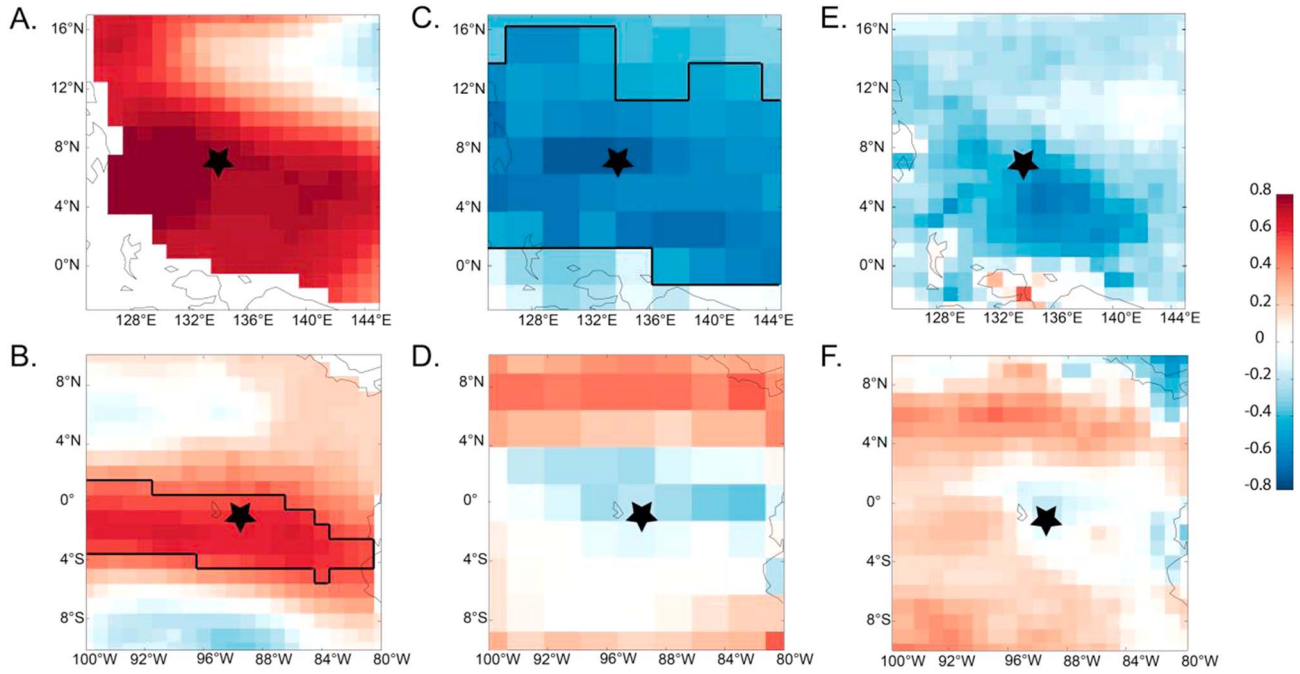

Figure 6. Correlation maps (Spearman rank) of monthly averaged $\delta^{18}O_{sw}$, gridded Argo mixed layer salinity, GPCP2.3 precipitation, and WHOI OAflux evaporation: (a) Palau $\delta^{18}O_{sw}$ and salinity. (b) Galápagos $\delta^{18}O_{sw}$ and salinity. (c) Palau $\delta^{18}O_{sw}$ and precipitation. (d) Galápagos $\delta^{18}O_{sw}$ and precipitation. (e) Palau $\delta^{18}O_{sw}$ and evaporation. (f) Galápagos $\delta^{18}O_{sw}$ and evaporation. Site locations are indicated by stars. Black outlined areas are significant at the 95% confidence level after accounting for autocorrelation via effective sample size and test multiplicity with the false discovery rate method [*Benjamini and Hochberg*, 1995; *Dawdy and Matalas*, 1964].

Both Galápagos and Palau $\delta^{18}O_{sw}$ are strongly correlated with regional salinity, with the strongest correlation focused on the equator around the Galápagos, and to the west of Palau, respectively (Figures 6a–6b). Due to the short length of the time series, high autocorrelation, and test multiplicity, we are unable to reject the null hypothesis at the 5% level for Palau. Palau $\delta^{18}O_{sw}$ is significantly correlated with regional precipitation, with more precipitation coincident with lower $\delta^{18}O_{sw}$ (Figure 6c). There is no significant correlation with precipitation in the eastern equatorial Pacific and Galápagos $\delta^{18}O_{sw}$ (Figure 6d), similar to the outcome of local correlations provided in Table 2. There is also no significant correlation between either Palau or Galápagos $\delta^{18}O_{sw}$ and evaporation (Figures 6e–6f), although similar to salinity, we cannot reject the null hypothesis due to the short time series and high spatial resolution of the gridded evaporation data set. Stronger correlations between evaporation and $\delta^{18}O_{sw}$ are found in regions more remote from the Galápagos, suggesting the possibility that advection of evaporated, high $\delta^{18}O_{sw}$ surface waters from the south or north could contribute to high $\delta^{18}O_{sw}$ locally. However, longer time series are required to adequately test this hypothesis.

4.4. Forward Modeling Coral $\delta^{18}O$ Using Local $\delta^{18}O_{sw}$-Salinity Relationships

Interpretation of coral $\delta^{18}O$ ($\delta^{18}O_c$) is confounded by the combined influences of both SST and $\delta^{18}O_{sw}$ on $\delta^{18}O_c$ values. With adequate characterization of the $\delta^{18}O_c$-SST and $\delta^{18}O_{sw}$-salinity relationships, forward modeling can aid in the assessment of the relative influence of SST and $\delta^{18}O_{sw}$ on $\delta^{18}O_c$ [*Thompson et al.*, 2011]. In this section we develop annually resolved (1950–2008) pseudocorals using a forward proxy model for $\delta^{18}O_c$. We use annual HadISST1.1 [*Rayner et al.*, 2003] and Delcroix sea surface salinity [*Delcroix et al.*, 2011] for each site and coefficients that express the relationship between both SST and $\delta^{18}O_c$ as well as salinity and $\delta^{18}O_{sw}$, following *Thompson et al.* [2011]. We use the HadISST1.1 and Delcroix data sets given the shorter length of the AVHRR SST and Argo data sets previously analyzed. We calculate annual $\delta^{18}O_c$ using the $\delta^{18}O_c$-SST coefficient of -0.22‰/°C and local $\delta^{18}O_{sw}$-salinity slopes as well as the pan tropical Pacific $\delta^{18}O_{sw}$-salinity slope of 0.27‰/psu (converting from VSMOW to VPDB by multiplying by 0.97). The fraction of $\delta^{18}O_c$ variance due to $\delta^{18}O_{sw}$ variability (fraction seawater, F_{sw}), is calculated following equation (2) in *Russon et al.* [2013].

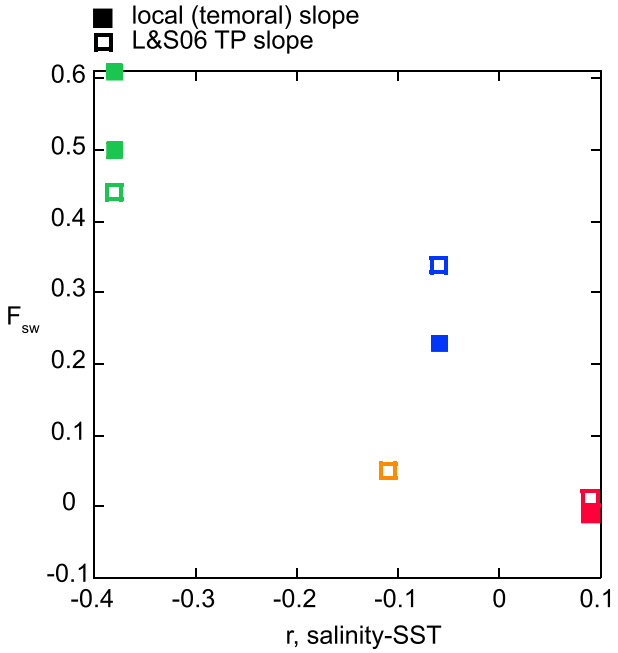

Figure 7. F_{sw} in annual modeled $\delta^{18}O_c$ and correlation coefficients between annual sea surface salinity and HadSST1.1 for each site, 1950–2008. Open squares show F_{sw} calculated with the pantropical Pacific $\delta^{18}O_{sw}$-salinity slope of 0.27‰/psu, filled squares show F_{sw} calculated with local $\delta^{18}O_{sw}$-salinity slopes. Squares are color coded by site. Green: Palau, blue: Manus, orange: Kiritimati, and red: Galápagos.

We find F_{sw} is highest at Manus and Palau, the two western tropical Pacific sites (Figure 7). This finding is similar to model results in *Russon et al.* [2013]. Here, $\delta^{18}O_{sw}$ likely has a large impact on $\delta^{18}O_c$ due to the strong hydrologic cycle in the region, leading to greater variability in P-E and $\delta^{18}O_{sw}$. F_{sw} is 11% higher at Manus when using the pantropical Pacific slope of 0.27‰/psu versus the local slope of 0.20‰/psu. F_{sw} is 6–17% lower at Palau if using the pantropical Pacific slope versus the local slopes of 0.32 and 0.42‰/psu. At these two sites, there is a negative correlation between $\delta^{18}O_{sw}$ and SST, consistent with freshening induced by SST warming. However, this correlation is insignificant at Manus ($r = -0.06$, $N = 58$, $p = 0.65$). Thus, at Manus, $\delta^{18}O_{sw}$ influences $\delta^{18}O_c$ and does so independently of SST. At Palau, $\delta^{18}O_{sw}$ influences $\delta^{18}O_c$, but in the same direction as SST—that is, warmer SST and lower $\delta^{18}O_{sw}$ both produce lower $\delta^{18}O_c$ values.

F_{sw} is near 0, indicating that $\delta^{18}O_{sw}$ has little impact on $\delta^{18}O_c$ in the Galápagos and Kiritimati datasets, where SST contributes the majority of $\delta^{18}O_c$ variance. Additionally, F_{sw} decreases by only 2% when substituting the local Galápagos $\delta^{18}O_{sw}$-salinity slope for the pantropical Pacific slope. Salinity is not significantly correlated with SST at Kiritimati ($r = -0.11$, $N = 58$, $p = 0.41$) and Galápagos $r = 0.09$, $N = 58$, $p = 0.50$). That is, freshening does not occur with warming on annual time scales from 1950 to 2008. Thus, in the eastern tropical Pacific, $\delta^{18}O_c$ can be more confidently used as a proxy for SST and differences in local versus tropical Pacific-wide $\delta^{18}O_{sw}$-salinity slopes do not strongly impact $\delta^{18}O_c$. However, our results stress the need for caution when considering $\delta^{18}O_c$ a proxy for SST in the western tropical Pacific.

5. Conclusions

We find significant differences in the temporal and spatial $\delta^{18}O_{sw}$-salinity relationship at four sites across the tropical Pacific. Higher slopes in the western tropical Pacific relative to a lower slope in the eastern tropical Pacific is apparent in both the observations and isotope-enabled model simulations. This may be a result of a stronger hydrologic cycle and lower $\delta^{18}O_p$ in the western Pacific associated with greater moisture convergence. We find that the local spatial $\delta^{18}O_{sw}$-salinity relationship is similar to the temporal $\delta^{18}O_{sw}$-salinity relationship at Manus and Galápagos over the time period investigated. At Palau, we observe differences in the temporal $\delta^{18}O_{sw}$-salinity slope from 1998 to 2000 and from 2013 to 2016. The Palau observations highlight the importance of interannual variability in the $\delta^{18}O_{sw}$-salinity relationship and the need for temporal records of $\delta^{18}O_{sw}$ and salinity that span many years at high temporal resolution (weekly to monthly).

Comparison of $\delta^{18}O_{sw}$ time series to key ocean and atmospheric variables emphasizes the importance of regional isotope-enabled ocean models for accurate $\delta^{18}O$ data-model comparison, as multiple factors, including precipitation, evaporation, upwelling, and meridional and zonal currents influence $\delta^{18}O_{sw}$. These results have implications for interpretation of $\delta^{18}O_{sw}$ and proxy system modeling of $\delta^{18}O$ in paleocean proxies. Broadly, our results indicate that use of the pantropical Pacific $\delta^{18}O_{sw}$-salinity coefficients may

overestimate or underestimate the contribution of $\delta^{18}O_{sw}$ variance to proxy carbonate $\delta^{18}O$ variance. In the western tropical Pacific, where $\delta^{18}O_{sw}$ more strongly influences coral $\delta^{18}O$ variance, applying the basin-wide slope leads to an overestimate of the contribution of $\delta^{18}O_{sw}$ to coral $\delta^{18}O$ variance at Manus, and an underestimation of the contribution of $\delta^{18}O_{sw}$ to coral $\delta^{18}O$ variance at Palau. Moreover, the strength of the relationship between salinity and SST is weak at all sites and insignificant at Manus, Galápagos, and Kiritimati. Thus, at Manus, not only does $\delta^{18}O_{sw}$ influence coral $\delta^{18}O$, but does so independently of SST. At Palau, both $\delta^{18}O_{sw}$ and SST contribute to lower $\delta^{18}O_c$ values, and $\delta^{18}O_{sw}$ thus enhances the signal of SST variance in $\delta^{18}O_c$. Thus, interpreting western tropical Pacific $\delta^{18}O_c$ values as proxies for SST is not ideal, whereas such an approach can be done with greater confidence in the central and eastern tropical Pacific.

Acknowledgments

We are grateful for the dedicated water samplers who enabled this research: Lori J. Bell and Gerda Ucharm of the Coral Reef Research Foundation, Palau; Rosa Maritza Motoche González and the Fuerza Aérea Ecuatoriana, Santa Cruz, Galápagos, Ecuador; Taonateiti Kabiri and the students of Tennessee Primary School, London, Kiritimati; and the Manus Weather Observers, U.S. Department of Energy ARM Climate Research Facility, Manus, Papua New Guinea. We would like to thank the Galápagos National Park, the Kiritimati Ministry of Environment Lands and Agricultural Development for sample permits, and the Charles Darwin Research Station for logistical support. Funding sources for this work includes NSF-AGS-PF 1049664 to J.L.C., NSF P2C2-1203785 to K.M.C., J.L.C., and D.N. This research was also supported by the Office of Biological and Environment Research of the U.S. Department of Energy as part of the Atmospheric Radiation Measurement Climate Research Facility. Isotope data are available as supporting information associated with the manuscript.

References

Adkins, J. F., K. McIntyre, and D. P. Schrag (2002), The salinity, temperature, and $\delta^{18}O$ of the glacial deep ocean, *Science*, *298*(5599), 1769–1773.

Adler, R. F., et al. (2003), The version-2 global precipitation climatology project (GPCP) monthly precipitation analysis (1979–present), *J. Hydrometeorol.*, *4*(6), 1147–1167.

Alibert, C., and M. T. McCulloch (1997), Strontium/calcium ratios in modern porites corals from the Great Barrier Reef as a proxy for sea surface temperature: Calibration of the thermometer and monitoring of ENSO, *Paleoceanography*, *12*(3), 345–363.

Argo (2000), Argo float data and metadata from Global Data Assembly Centre (Argo GDAC), *SEANOE*.

Beck, J. W., J. Recy, F. Taylor, R. L. Edwards, and G. Cabioch (1997), Abrupt changes in early Holocene tropical sea surface temperature derived from coral records, *Nature*, *385*(6618), 705–707.

Benjamini, Y., and Y. Hochberg (1995), Controlling the false discovery rate: A practical and powerful approach to multiple testing, *J. R. Stat. Soc. B. Method.*, *57*, 289–300.

Benway, H. M., and A. C. Mix (2004), Oxygen isotopes, upper-ocean salinity, and precipitation sources in the eastern tropical Pacific, *Earth Planet. Sci. Lett.*, *224*(3–4), 493–507.

Bonjean, F., and G. S. E. Lagerloef (2002), Diagnostic model and analysis of the surface currents in the tropical Pacific Ocean, *J. Phys. Oceanogr.*, *32*(10), 2938–2954.

Conroy, J. L., K. M. Cobb, and D. Noone (2013), Comparison of precipitation isotope variability across the tropical Pacific in observations and SWING2 model simulations, *J. Geophys. Res. Atmos.*, *118*, 1–26, doi:10.1002/jgrd.50412.

Conroy, J. L., K. M. Cobb, J. Lynch-Stieglitz, and P. J. Polissar (2014), Constraints on the salinity–oxygen isotope relationship in the central tropical Pacific Ocean, *Mar. Chem.*, *161*, 26–33.

Conroy, J. L., D. Noone, K. M. Cobb, J. W. Moerman, and B. L. Konecky (2016), Paired stable isotopologues in precipitation and vapor: A case study of the amount effect within western tropical Pacific storms, *J. Geophys. Res. Atmos.*, *121*, 3290–3303, doi:10.1002/2015JD023844.

Dawdy, D. R., and N. C. Matalas (1964), Statistical and probability analysis of hydrologic data, Part III: Analysis of variance, covariance and time series, in *Handbook of Applied Hydrology, a Compendium of Water-Resources Technology*, edited by V. T. Chow, pp. 8.68–68.90, McGraw-Hill, New York.

Delaygue, G., E. Bard, C. Rollion, J. Jouzel, M. Stievenard, J. C. Duplessy, and G. Ganssen (2001), Oxygen isotope/salinity relationship in the northern Indian Ocean, *J. Geophys. Res.*, *106*(C3), 4565–4574.

Delcroix, T., G. Alory, S. Cravatte, T. Corrège, and M. McPhaden (2011), A gridded sea surface salinity data set for the tropical Pacific with sample applications (1950–2008), *Deep Sea Res., Part I*, *58*(1), 38–48.

Durack, P. J., S. E. Wijffels, and R. J. Matear (2012), Ocean salinities reveal strong global water cycle intensification during 1950–2000, *Science*, *336*(6080), 455–458.

Evans, M. N., S. E. Tolwinski-Ward, D. M. Thompson, and K. J. Anchukaitis (2013), Applications of proxy system modeling in high resolution paleoclimatology, *Quat. Sci. Rev.*, *76*, 16–28.

Fairbanks, R. G., M. N. Evans, J. L. Rubenstone, R. A. Mortlock, K. Broad, M. D. Moore, and C. D. Charles (1997), Evaluating climate indices and their geochemical proxies measured in corals, *Coral Reefs*, *16*, S93–S100.

Fine, R. A., R. Lukas, F. M. Bingham, M. J. Warner, and R. H. Gammon (1994), The western equatorial Pacific: A water mass crossroads, *J. Geophys. Res.*, *99*, 25,063–25,080, doi:10.1029/94JC02277.

Hasson, A. E. A., T. Delcroix, and R. Dussin (2013), An assessment of the mixed layer salinity budget in the tropical Pacific Ocean. Observations and modelling (1990–2009), *Ocean Dyn.*, *63*(2–3), 179–194.

Holloway, M. D., L. C. Sime, J. S. Singarayer, J. C. Tindall, and P. J. Valdes (2016), Reconstructing paleosalinity from $\delta^{18}O$: Coupled model simulations of the Last Glacial Maximum, Last Interglacial and late Holocene, *Quat. Sci. Rev.*, *131*, 350–364.

Huffman, G. J., D. T. Bolvin, E. J. Nelkin, D. B. Wolff, R. F. Adler, G. Gu, Y. Hong, K. P. Bowman, and E. F. Stocker (2007), The TRMM multisatellite precipitation analysis (TMPA): Quasi-global, multiyear, combined-sensor precipitation estimates at fine scales, *J. Hydrometeorol.*, *8*(1), 38–55.

Kısakürek, B., A. Eisenhauer, F. Böhm, D. Garbe-Schönberg, and J. Erez (2008), Controls on shell Mg/Ca and Sr/Ca in cultured planktonic foraminiferan, *Globigerinoides ruber* (white), *Earth Planet. Sci. Lett.*, *273*(3–4), 260–269.

Kuroda, Y. (2000), Variability of currents off the northern coast of New Guinea, *J. Oceanogr.*, *56*(1), 103–116.

Lea, D. W., T. A. Mashiotta, and H. J. Spero (1999), Controls on magnesium and strontium uptake in planktonic foraminifera determined by live culturing, *Geochim. Cosmochim. Acta*, *63*(16), 2369–2379.

Lee, T., G. Lagerloef, M. M. Gierach, H.-Y. Kao, S. Yueh, and K. Dohan (2012), Aquarius reveals salinity structure of tropical instability waves, *Geophys. Res. Lett.*, *39*, L12610, doi:10.1029/2012GL052232.

Leech, P. J., J. Lynch-Stieglitz, and R. Zhang (2013), Western Pacific thermocline structure and the Pacific marine Intertropical Convergence Zone during the Last Glacial Maximum, *Earth Planet. Sci. Lett.*, *363*, 133–143.

LeGrande, A. N., and G. A. Schmidt (2006), Global gridded data set of the oxygen isotopic composition in seawater, *Geophys. Res. Lett.*, *33*, L12604, doi:10.1029/2006GL026011.

LeGrande, A. N., and G. A. Schmidt (2011), Water isotopologues as a quantitative paleosalinity proxy, *Paleoceanography*, *26*, PA3225, doi:10.1029/2010PA002043.

Morimoto, M., O. Abe, H. Kayanne, N. Kurita, E. Matsumoto, and N. Yoshida (2002), Salinity records for the 1997–98 El Nino from Western Pacific corals, *Geophys. Res. Lett.*, *29*(11), 1540, doi:10.1029/2001GL013521.

Nurhati, I. S., K. M. Cobb, and E. Di Lorenzo (2011), Decadal-scale SST and salinity variations in the central tropical Pacific: Signatures of natural and anthropogenic climate change, *J. Clim.*, *24*(13), 3294–3308.

Rayner, N. A., D. E. Parker, E. B. Horton, C. K. Folland, L. V. Alexander, D. P. Rowell, E. C. Kent, and A. Kaplan (2003), Global analyses of sea surface temperature, sea ice, and night marine air temperature since the late nineteenth century, *J. Geophys. Res.*, *108*(D14), 4407, doi:10.1029/2002JD002670.

Reynolds, R. W., T. M. Smith, C. Liu, D. B. Chelton, K. S. Casey, and M. G. Schlax (2007), Daily high-resolution-blended analyses for sea surface temperature, *J. Clim.*, *20*(22), 5473–5496.

Roberts, J., J. Gottschalk, L. C. Skinner, V. L. Peck, S. Kender, H. Elderfield, C. Waelbroeck, N. V. Riveiros, and D. A. Hodell (2016), Evolution of South Atlantic density and chemical stratification across the last deglaciation, *Proc. Natl. Acad. Sci. U.S.A.*, *113*(3), 514–519, doi:10.1073/pnas.1511252113.

Rohling, E. J., and G. R. Bigg (1998), Paleosalinity and $\delta^{18}O$: A critical assessment, *J. Geophys. Res.*, *103*(C1), 1307–1318, doi:10.1029/97JC01047.

Russon, T., A. Tudhope, G. Hegerl, M. Collins, and J. Tindall (2013), Inter-annual tropical Pacific climate variability in an isotope-enabled CGCM: Implications for interpreting coral stable oxygen isotope records of ENSO, *Clim. Past*, *9*(4), 1543–1557.

Rustic, G. T., A. Koutavas, T. M. Marchitto, and B. K. Linsley (2015), Dynamical excitation of the tropical Pacific Ocean and ENSO variability by Little Ice Age cooling, *Science*, *350*(6267), 1537–1541.

Stevenson, S., B. Powell, M. Merrifield, K. Cobb, J. Nusbaumer, and D. Noone (2015), Characterizing seawater oxygen isotopic variability in a regional ocean modeling framework: Implications for coral proxy records, *Paleoceanography*, *30*, 1573–1593, doi:10.1002/2015PA002824.

Stott, L., K. Cannariato, R. Thunell, G. H. Haug, A. Koutavas, and S. Lund (2004), Decline of surface temperature and salinity in the western tropical Pacific Ocean in the Holocene epoch, *Nature*, *431*(7004), 56–59.

Thompson, D. M., T. R. Ault, M. N. Evans, J. E. Cole, and J. Emile-Geay (2011), Comparison of observed and simulated tropical climate trends using a forward model of coral d(18)O, *Geophys. Res. Lett.*, *38*, L14706, doi:10.1029/2011GL048224.

Thompson, D. M., T. R. Ault, M. N. Evans, J. E. Cole, J. Emile-Geay, and A. N. LeGrande (2013), Coral-model comparison highlighting the role of salinity in long-term trends, *PAGES News*, *21*(2), 60–61.

van Geldern, R., and J. A. C. Barth (2012), Optimization of instrument setup and post-run corrections for oxygen and hydrogen stable isotope measurements of water by isotope ratio infrared spectroscopy (IRIS), *Limnol. Oceanogr. Methods*, *10*, 1024–1036.

Wellington, G. M., R. B. Dunbar, and G. Merlen (1996), Calibration of stable oxygen isotope signatures in Galapagos corals, *Paleoceanography*, *11*(4), 467–480.

Wolanski, E., P. Colin, J. Naithani, E. Deleersnijder, and Y. Golbuu (2004), Large amplitude, leaky, island-generated, internal waves around Palau, Micronesia, *Estuarine Coastal Shelf Sci.*, *60*(4), 705–716.

Yu, L. S., and R. A. Weller (2007), Objectively analyzed air-sea heat fluxes for the global ice-free oceans (1981–2005), *Bull. Am. Meteorol. Soc.*, *88*(4), 527–539, doi:10.1175/BAMS-88-4-527.